sustainability

MDPI

Article

Remote Sensing Land Use Evolution in Earthquake-Stricken Regions of Wenchuan County, China

Junmei Kang [1], Zhihua Wang [2,3,*], Hongbin Cheng [1], Jun Wang [1] and Xiaoliang Liu [2,3]

[1] The Second Monitoring and Application Center, China Earthquake Administration, Xi'an 710054, China
[2] State Key Laboratory of Resources and Environmental Information System, Institute of Geographic Sciences and Natural Resources Research, Chinese Academy of Sciences, Beijing 100101, China
[3] College of Resources and Environment, University of Chinese Academy of Sciences, Beijing 100049, China
* Correspondence: zhwang@lreis.ac.cn

Abstract: Earthquakes and their secondary geological disasters have a certain impact on the land cover, which leads to the degradation of the ecological environment and the stability of the ecosystem. At present, there are few studies on the spatial–temporal evolution characteristics of land-use change in earthquake-stricken regions, especially the lack of quantitative evaluation of the impact of earthquakes on land use at the micro-scale. The "5·12" Wenchuan ms8.0 earthquake caused serious damage to the surface resources in the disaster area. The study on the spatial–temporal evolution characteristics of land-use change in the disaster area can provide a reference for the remote sensing dynamic monitoring of the ecological environment. Therefore, based on geographical big data, this paper used a land-use comprehensive degree index, land-use transfer matrix, and landscape ecological index to explore and analyze the spatial–temporal evolution characteristics of land use in Wenchuan County before and after the earthquake. The results showed that the types of cropland, forest, built-up, and bare land changed greatly before and after the earthquake. During the earthquake recovery period, the comprehensive index of land use in the study area basically showed an increasing trend. Under the effect of artificial measures and natural restoration, land use was continuously improved, and vegetation was restored well. After 2008, the Patch Density (PD) and Landscape Shape Index (LSI) values of most landscape types decreased, and the Aggregation Index (AI) values increased, indicating that the ecological environment of the whole region showed a benign development in the post-earthquake period. The results not only contribute to the establishment of scientific ecological environment management in earthquake-stricken regions but also contribute to the formulation of long-term ecological environment monitoring and ecological restoration planning according to the law of land-use change.

Keywords: remote sensing; Wenchuan earthquake; land use; landscape pattern; spatial–temporal evolution

Citation: Kang, J.; Wang, Z.; Cheng, H.; Wang, J.; Liu, X. Remote Sensing Land Use Evolution in Earthquake -Stricken Regions of Wenchuan County, China. *Sustainability* **2022**, *14*, 9721. https://doi.org/10.3390/su14159721

Academic Editor: Antonio Miguel Martínez-Graña

Received: 8 July 2022
Accepted: 5 August 2022
Published: 7 August 2022

1. Introduction

Earthquake disasters not only cause huge casualties and property losses [1–4] but also destroy a large number of forest, cropland, urban, and other land types [5,6] due to secondary disasters caused by earthquakes and landslides, mud-rock flows, etc., which greatly change the land use types in the disaster regions, thus causing certain damage to the ecological environment [7–10]. Many countries have actively carried out disaster prevention and mitigation activities to effectively improve disaster response capacity. For example, data released by the Indonesian state show that since 2022, Indonesia has suffered 873 natural disasters, including floods, strong winds, landslides, etc., and more than 4.13 million people have been affected by the disasters. The direct economic loss caused by natural disasters to Indonesia is as high as 28.8 trillion rupiahs every year. In the past 15 years, natural disasters in China have caused direct economic losses of nearly 200 billion yuan every year.

Therefore, the public nature and public welfare features of natural disaster relief cause the basic position of public financial expenditure to appear extremely important. For example, the Chinese government invested a total of 82.514 billion yuan in earthquake relief funds after the 2008 Wenchuan earthquake in China. As one of the most basic and important natural resources, land resources are a key field and the most basic material basis, energy sources, space carriers, and constituent element for realizing the sustainable development of the economy and society and the harmonious development of man and nature. It is a major strategic issue concerning national economic and social development [11–14].

Remote sensing technology is a very important contemporary science and technology and has a simple acquisition, low price, multi-scale, rich spectral information, ease of operation, and other advantages that other technologies cannot compare [15–18]; it has become an important technical means and methods of geology, ecology, disaster science and other research [19–22]. Remote sensing images can accurately record the actual situation of earthquake disasters, provide specific and effective information for disaster warning and ecological environment monitoring, and provide data support for rapid evaluation of the damage caused by disasters and scientific decision-making, which is a reliable technical means at present [23–25].

The "5·12", 2008 Wenchuan ms8.0 earthquake caused serious damage to the surface resources in earthquake-stricken regions. Some scholars began to pay attention to the evolution of secondary disasters in earthquake-stricken regions and their impact on land-use change and carried out a series of research works from different perspectives [26,27]. Cui et al. [28] studied the mechanism of the Wenchuan earthquake, gathered statistics, and analyzed landslides after the earthquake. It was found that the loose material generated by the earthquake was the main material source of debris flow activities after the earthquake, and strong surface disturbance and large-scale vegetation destruction would intensify erosion and flood peak formation. Nath et al. [29] analyzed the changes in land use in Dujiangyan city from 2007 to 2018 from the perspective of an environmental risk assessment and found that urban land, cropland, and forests were the most affected land types and suggested that future urban construction and development should avoid active fault areas. Yang et al. [30] analyzed the distribution of landslides and the rebuilt houses after the Wenchuan earthquake from the perspective of restoration and reconstruction and found that the new landslides and houses tended to move to regions with low elevation, gentle slopes, and were close to river channels. In addition, the destruction and restoration of vegetation in earthquake-stricken regions after the Wenchuan earthquake has also attracted the attention of many researchers. Some scholars have evaluated the destruction and restoration of vegetation in earthquake-stricken regions based on remote sensing methods. Wang et al. [31] fully considered the dynamic change process of vegetation restoration and defined the Count of Outliers Index (COI) to identify difficult regions of vegetation restoration based on Normalized Difference Vegetation Index (NDVI) time series data. Zhang et al. [32] defined the Difference Measurement Index (DMI) to evaluate the vegetation restoration state through comparative statistical analysis with the historical vegetation state, overcoming the influence of the previous index on the fluctuation of vegetation phenology between years. Liu et al. [33] calculated the ecological recovery capacity of the severely affected regions of the Wenchuan earthquake by fitting the curve of recovery rate and time with Moderate-Resolution Imaging Spectroradiometer Enhanced Vegetation Index (MODIS-EVI) data. The results showed that 44.2% of the damaged regions had been restored and suggested that priority should be given to the construction of damaged regions near roads, rivers, and mining operations. Among them, the area of vegetation restoration is 187.40 km^2. Of course, some scholars have carried out monitoring research on land use and other information concerning earthquake-stricken regions abroad based on remote sensing technology [34]. For example, Balamurugan et al. [35] monitored land-use change on the western coast of Gujarat, India, based on remote sensing and geographic information technology. The results show that the output shows a decline in the agricultural and scrubland, an increase in fallow land and saltpans, and exponential

increases in built-up areas in the area. Thilagavathi et al. [36] took Salem Chalk Hills and South India as their research area and analyzed the process of human-induced landscape transformation in the mine-affected areas of Chalk Hills, Salem, by interpreting Landsat TM and IRS P6 LISS IV MX satellite image data for the year 2002 and 2012 using the Geographic Information System (GIS). Ishihara et al. [37] took the 2011 east Japan earthquake as their research object and created a precise land-cover map for the years 2013–2015 post-disaster with a 30 m spatial resolution using Landsat 8 with Operational Land Imager (OLI) to evaluate the changes in land cover induced by the disaster.

Based on the above research progress, it can be found that in the early stage of the research on the earthquake-stricken regions, scholars at home and abroad focused on the mechanism of earthquake-induced occurrence, the analysis of seismic damage to buildings in the earthquake-stricken regions, and the distribution of earthquake-induced landslides, collapses, and other geological disasters. With the development of remote sensing technology, scholars at home and abroad have used remote sensing technology as a means to study the impact of earthquakes on land resource utilization, ecosystem services, ecosystem carrying capacity, and other aspects, and the risk assessment of geological disasters in earthquake-stricken regions from a macro-regional perspective. However, there are few studies on the spatial–temporal evolution characteristics of land-use change in earthquake-stricken regions, especially the lack of quantitative evaluation of the impact of earthquakes on land use at the micro-scale.

The Wenchuan earthquake was a natural disaster with a strong earthquake feeling, wide spread, and a high degree of damage [38]. The Wenchuan earthquake inflicted not only heavy losses on people's finances, life, and property but also triggered secondary geological disasters, such as landslides, collapses, and mud–rock flows. It aggravated regional soil erosion, reduced biodiversity, increased resource consumption, and degraded ecological functions, posing a threat to human survival and sustainable social and economic development [39–42]. The land cover of the cropland and forests in the earthquake-stricken regions was destroyed, resulting in the destruction of the regional ecosystem and the serious degradation of the ecological environment, resulting in an imbalance of the stability of the ecosystem [43–46]. After the earthquake, people's focus was mainly on infrastructure, economy, water resources, etc., and it is easy to ignore the ecological environment deterioration caused by land-cover destruction, thus posing a threat to human production and development.

In summary, this paper takes Wenchuan County, Sichuan Province, as the research area and obtained land-use data before the earthquake (2007), earthquake year (2008), the middle period of earthquake recovery (2014) and the late period of earthquake recovery (2020) and other auxiliary data based on geographical big data. The spatial–temporal evolution characteristics of land use in Wenchuan County before and after the earthquake were analyzed comprehensively from the methods of land use degree, land transfer matrix, and the landscape index of quantitative evaluation of landscape patterns in landscape ecology; the driving mechanism of land-use change was discussed. The results of the earthquake-disaster region ecological environment remote sensing dynamic monitoring not only provide data support but also provide the regional, relevant decision-making departments with a timely and effective manner to provide the disaster region with land-use change data, which allows the ease of policies and measures, and the administrative department can improve government control over land-resource-utilization efficiency, and promote the earthquake-stricken region's ecological environment monitoring and recovery process.

2. Materials

2.1. Study Area

Wenchuan County (30°45′~31°43′ N, 102°51′~103°44′ E) is located in Tibetan Qiang Autonomous Prefecture of Ngawa, Sichuan Province, China. It borders Dujiangyan city and Pengzhou city in the east, Lushan County, Dayi County, and Chongzhou city in the

south, Li County, Xiaojin County, and Baoxing County in the west, and Mao County in the north, with a total area of 4084 km^2. The terrain of Wenchuan County tilts from northwest to southeast, with a relative elevation difference of 3000 m and an average elevation of 1326 m. The mountain of Wenchuan County is relatively steep; the terrain is relatively large, and the change of altitude affects the distribution of plant communities, thus forming different types of plant belts. The geological structure of Wenchuan County is complex; the strata are well developed, the magmatic rocks are widely distributed, and the structural transformation of the rock and soil mass is strong. The regional tectonic movement stress field causes the development of rock mass joints and fissures, lithology breakage, and structural plane development. Thus, the mechanical properties of the rock mass are greatly changed, which provides conditions for the development of geological disasters. The climate in Wenchuan County belongs to the Cw (warm temperate climate with a dry winter) in the Koppen–Geiger climate classification and decreases along with the terrain from northwest to southeast. The vertical climate zone is relatively complete, and the temperature is moderate. The average annual temperature in the area above 2000 m is 13.5~14.1 °C, the frost-free period is 247~269 d, and the rainfall is 528.7~1332.2 mm. Rivers in Wenchuan County mainly include the Minjiang River, and its tributaries are the Shoujiang River, Caopo River, and Zaguanao River. The tributaries at all levels are dendritic, rivers crisscross, and ravines crisscross. The geographical location of the study area is shown in Figure 1.

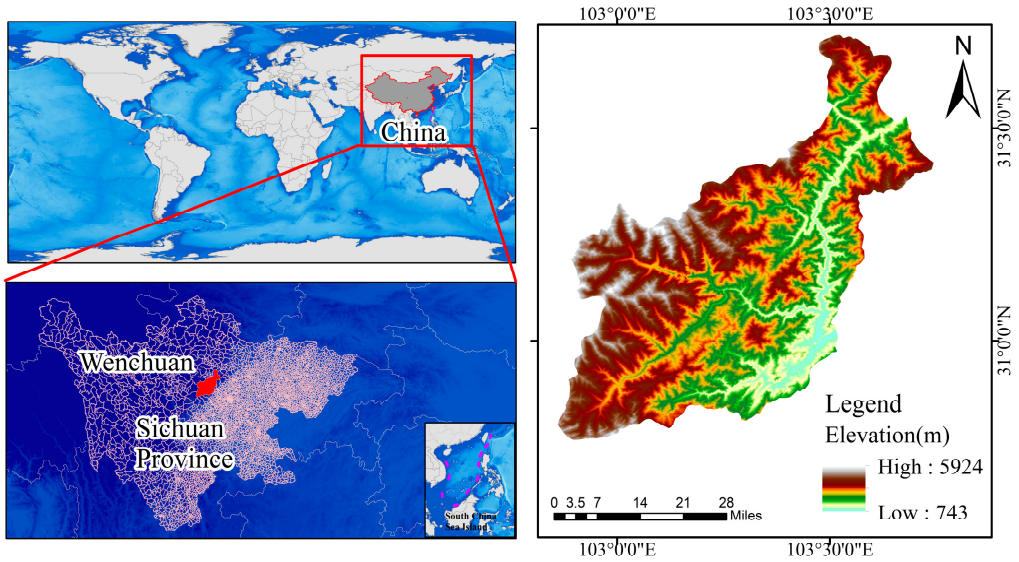

Figure 1. The geographical location of the study area.

2.2. Data and Preprocessing

The land-use data used in this study (pre-earthquake (2007), earthquake year (2008), mid-earthquake recovery (2014), and post-earthquake recovery (2020)) were derived from the annual 30m land-use data in China produced by Professor Xin Huang's team at Wuhan University [47] (https://zenodo.org/record/4417810#.YrpbL71BxPa (accessed on 6 January 2022)). These data were based on 335,709 Landsat images from the Google Earth Engine (GEE), combined with the automatic stabilization samples and visual interpretation samples of existing land-cover products, and the classification results were obtained by a random forest classifier. The WGS UTM projection was used as the reference frame for the analysis of this paper. Figure 2 shows the land-use data for each period in the study area.

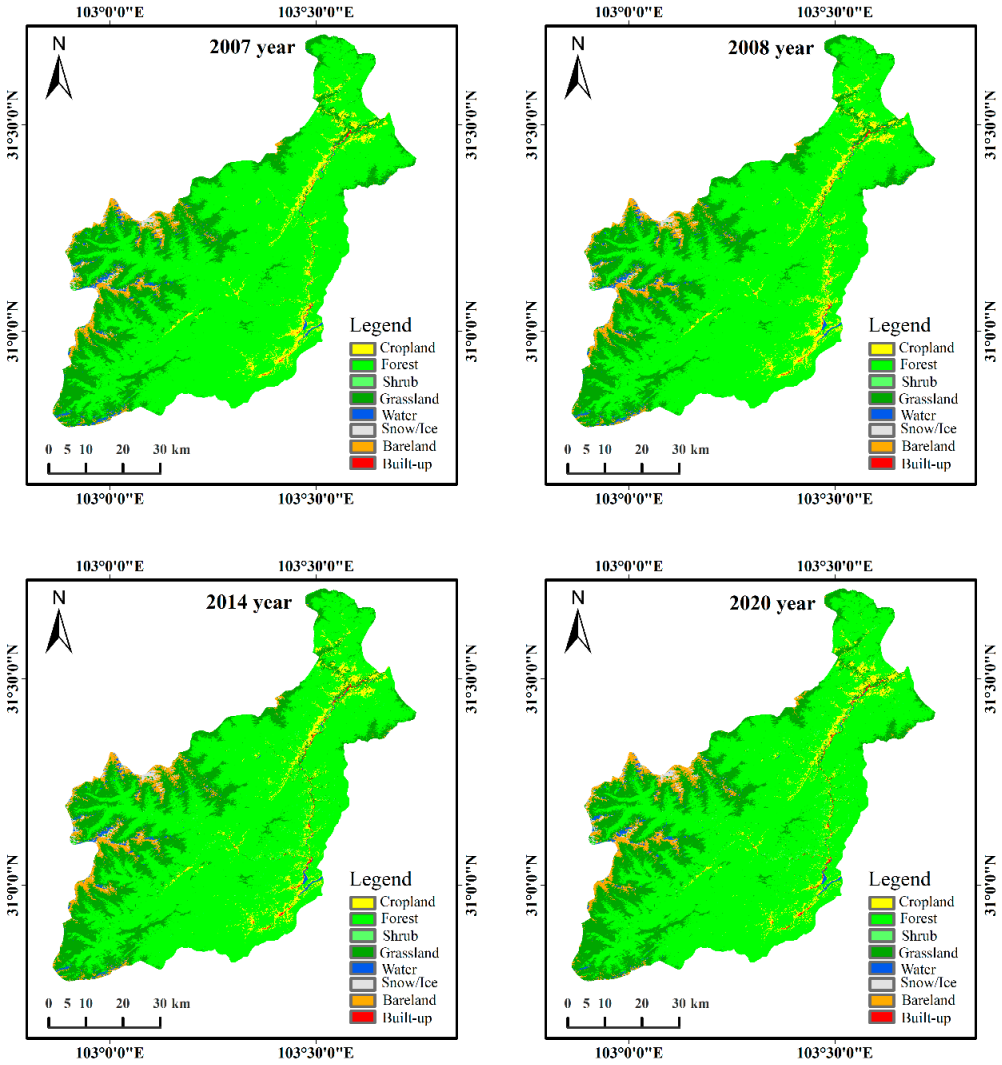

Figure 2. The spatial distribution of land use in different periods in the study area.

A confusion matrix is a commonly used precision evaluation method to calculate the consistency between the sample classification results and the real surface classification in the form of a matrix [48,49]. Based on the obfuscation matrix, the relevant indexes for evaluating the accuracy of the whole population and specific categories can be calculated [50]. In order to verify that the obtained land-use data met the research needs, we collected sample points in corresponding periods based on high-resolution images from Google Earth (Figure 3 is the collected sample point in 2020) and then evaluated the accuracy of the land-use data in various periods based on a confusion matrix. Table 1 shows the accuracy of the evaluation results. The results showed that the overall accuracy of the land-use data of the four periods is higher than 83%, and the kappa coefficient is higher than 0.75. According to the relationship of classification accuracy corresponding to different kappa values [51], the accuracy of the land-use data obtained in this paper is good, which me the research needs of this paper.

Table 1. Accuracy evaluation results of land-use data.

Year	2007	2008	2014	2020
OA (%)	83.68	83.25	85.90	86.12
Kappa	0.75	0.76	0.78	0.80

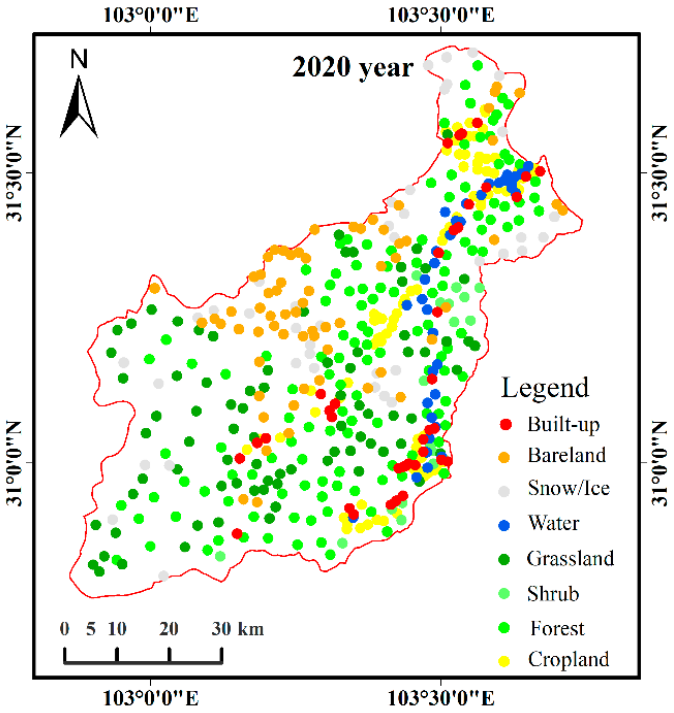

Figure 3. The spatial distribution of samples in 2020.

3. Methods

3.1. Comprehensive Index of Land Use Degree

The degree of land use can effectively reflect the depth and breadth of land development and utilization. It not only includes the change in land-use mode but also includes the change in land-use quantity and fully combines the natural attributes of land resources with the social attributes of human activities [52]. The degree of land use is a reflection of the scientificness and rationality of the land-use pattern, type, structure, and layout and is an important indicator of the regional ecological environment [53]. The land-use degree can be evaluated by the comprehensive index of land-use degree and its change rate, and the calculation formula is as follows:

$$I_a = 100 \times \sum_{i=1}^{n} A_i \times C_i \quad (1)$$

$$R = \frac{\sum_{i=1}^{n}(A_i \times C_{ib}) - \sum_{i=1}^{n}(A_i \times C_{ia})}{\sum_{i=1}^{n}(A_i \times C_{ia})} \times 100 \quad (2)$$

where, I_a represents the comprehensive index of land-use degree in the study area; A_i represents the grade index of grade i land-use degree in the study area; C_i represents the percentage of grade i land area in the study area; R represents the change rate of the land-use degree; C_{ib} and C_{ia} represent the area percentage of the study area in grade i land-use degree at time b and time a, respectively. If $\Delta I_{b-a} > 0$, this indicates that the land use in the study area is in the rising development stage; if $\Delta I_{b-a} < 0$, this indicates that land use in the study area is in a declining stage. The grading assignment for the land-use degree is shown in Table 2.

Table 2. Grading assignment of land use degree.

Land-Use Type	Bare Land, Snow/Ice	Forest, Grassland, Shrub, Water	Cropland	Built-Up
Grading index	1	2	3	4

3.2. Land Use Transfer Matrix

The land-use transfer matrix can not only provide the area of a certain land-use type to other land types in the current year but also provides the internal conversion information of land use between two time periods [54]. It can fully reflect the number, direction, and probability of the transfer of species in different regions under earthquake disturbance, which is of great significance to the study of the degree of ecological environment restoration in earthquake-stricken regions. The basic expression of the land-use transfer matrix is as follows:

$$P_{ij} = \begin{Bmatrix} P_{11} & P_{12}P_{13} & \cdots & P_{1n} \\ P_{21} & P_{22}P_{23} & \cdots & P_{2n} \\ \cdots & \cdots & \cdots & \cdots \\ P_{n1} & P_{n2}P_{n3} & \cdots & P_{nn} \end{Bmatrix} (i, j = 1, 2, 3, \cdots, n) \quad (3)$$

where, P_{ij} represents the area of the i-th land-use type converted to the j-th type of land-use type; n represents the number of land-use types; i and j represent the land-use types before and after transfer, respectively.

3.3. Landscape Ecological Index

A landscape index can quantitatively describe the structural composition and spatial configuration of a landscape. It is a widely used method for the quantitative description of a landscape pattern, as well as an important means for quantitative analysis of landscape patterns and dynamic changes in land-use data [55]. An earthquake and its secondary geological disasters' influence on landscape pattern change is a natural disturbance in the ecology, and post-disaster reconstruction is considered by some people to be a process of artificial interference, and the action of natural and artificial interference can cause changes to regional landscape elements; thus, light, water, and energy influence the absorption of nutrients and cause the original landscape pattern to change. Based on the analysis of the ecological significance of the existing landscape indexes, the selected landscape indexes include PD, LSI, and AI. The ecological significance of each landscape index is as follows [56]:

(1) PD: PD is a measure of landscape fragmentation, which can better reflect the characteristics of landscape heterogeneity. A smaller patch density corresponds to smaller landscape heterogeneity and fragmentation. In addition, the intensity and extensiveness of interactions among landscape elements can also be indirectly reflected by PD. The more active the landscape ecological process is, the higher the PD value is. The calculation formula of PD is as follows:

$$PD = \frac{N}{A}, PD > 0 \quad (4)$$

where, N represents the total number of patches in the landscape; A represents the total landscape area.

(2) LSI: LSI is a landscape index used to describe landscape pattern characteristics based on the shape of the landscape. The shape of the landscape is simple, which means that the LSI value is close to 1. If a square can be used to describe the landscape shape, the LSI value is 1. The larger the deviation between the landscape shape and square, the larger the LSI value. LSI is calculated as follows:

$$LSI = \frac{0.25E}{\sqrt{A}}, LSI \geq 1 \quad (5)$$

where, E represents the total length of all patch boundaries in the landscape; A represents the total landscape area.

(3) AI: AI is an important indicator when measuring landscape heterogeneity from the perspective of the connectivity between landscape patches. A small value of AI

means that patches in the landscape are scattered and fragmented. The AI calculation formula is as follows:

$$AI = \left[\frac{g_{ii}}{\max g_{ii}}\right] \times 100, 0 \le AI \le 100 \quad (6)$$

where, g_{ii} represents the number of similar connections between pixels of patch type i.

4. Results

4.1. Land Use Area Change

Figure 4 shows the spatial pattern distribution of the land-use area change of each township in the study area before and after the earthquake. Before and after the earthquake, the large variation of cropland type is mainly distributed in the east and north of the study area, which is also the main distribution area of cropland in the study area. Before the earthquake, the cropland area of Shuimo Town, Yingxiu Town, and Xuankou Town was 15.52 km^2, 8.39km^2, and 18.92 km^2, respectively. Due to the comprehensive impact of the earthquake and human activities, the cropland types recovered slowly in the late earthquake period. By 2020, the cropland area was 10.67 km^2, 4.70 km^2, and 12.03 km^2, respectively.

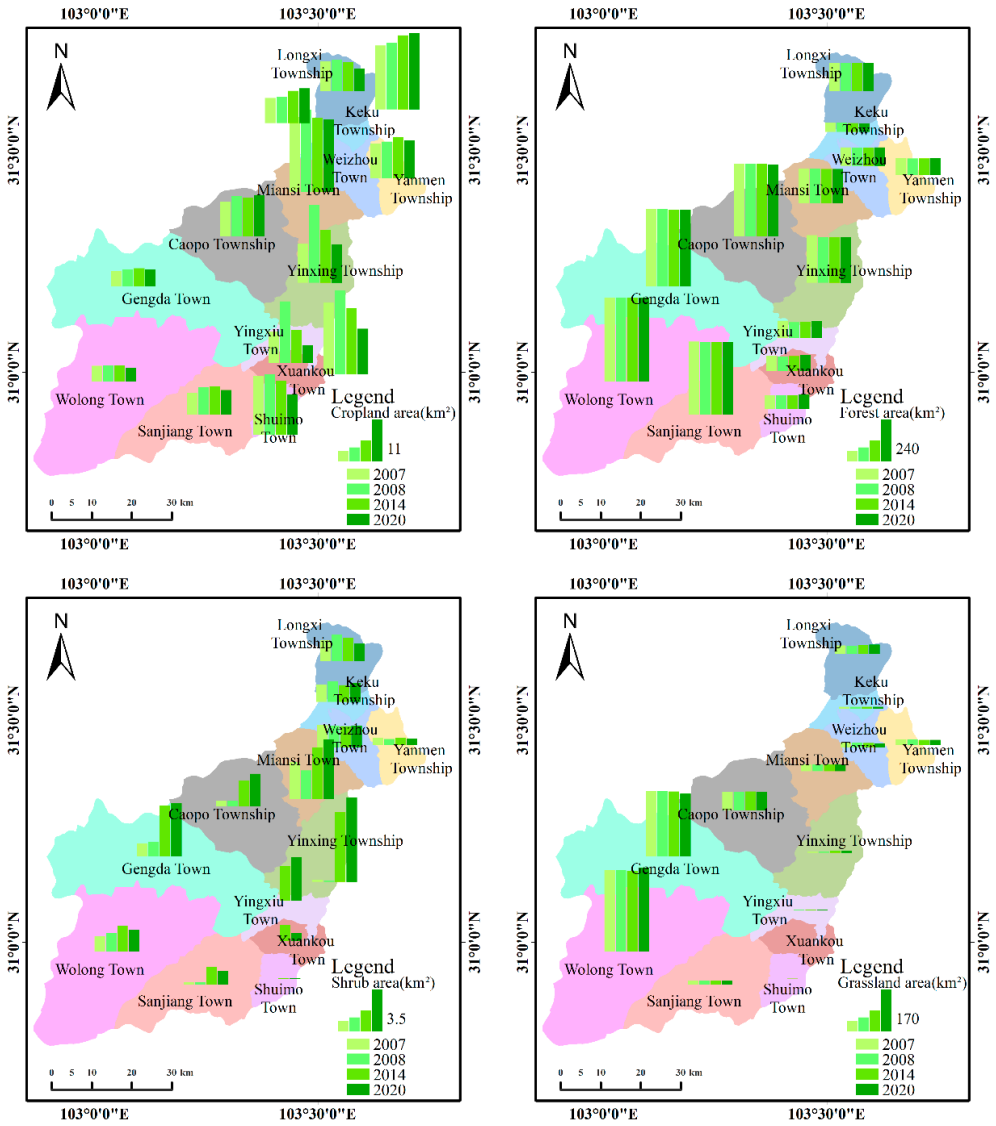

Figure 4. *Cont.*

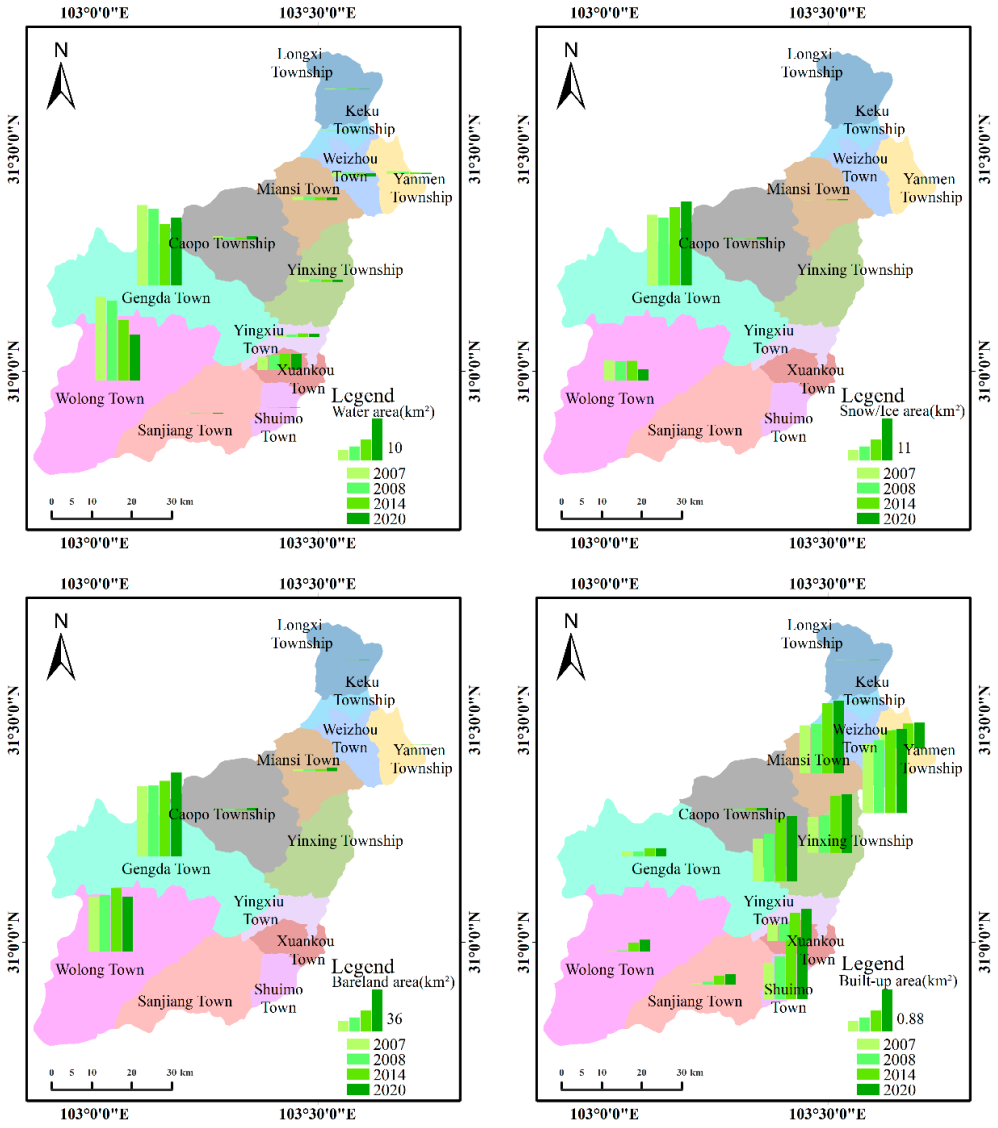

Figure 4. Spatial distribution of land-use area change before and after earthquake.

Regarding the forest type, in Yinxing Township, the area of forest type decreased from 272.98 km^2 in 2007 to 262.26 km^2 in 2008 and increased to 262.53 km^2 in 2020. Regarding the shrub type, the earthquake had a great influence in Miansi Town, Yanmen Township, Weizhou Town and Yinxing Township, and the shrub area decreased from 2007 to 2008. Regarding the grassland type, the area of grassland type in the study area changed slightly before and after the earthquake and showed a steady trend.

Gengda Town and Wolong Town were the main areas of the water-type areas affected by the earthquake. Gengda Town and Wolong Town's water area decreased from 19.43 km^2 and 20.36 km^2 in 2007 to 18.62 km^2 and 19.43 km^2 in 2008, respectively. Due to the influence of regional development, environment, climate, and other comprehensive factors, the water area in Gengda Town and Wolong Town was still lower than before the earthquake in the later period of earthquake recovery. The ice/snow was mainly distributed in Gengda Town in the study area; the area decreased from 19.27 km^2 in 2007 to 18.54 km^2 in 2008 due to the earthquake. The area of ice/snow increased gradually in the later period of the earthquake.

The bare land is mainly distributed in Gengda Town and Wolong Town in the study area. The bare land area mainly reflects the change of landslides. As the Wenchuan earthquake triggered a large number of landslides, Gengda Town and Wolong Town increased from 59.62 km^2 and 46.83 km^2 in 2007 to 60.53 km^2 and 48.14 km^2 in 2008,

respectively. After the earthquake recovery, the bare land area of Wolong Town gradually recovered to the level before the earthquake.

The change in built-up areas reflects the change in human activities. Before the earthquake, the economy in the study area was in a stage of rapid development, and the population was gradually increasing. The built-up area in the study area showed an overall growth trend. After the earthquake, a large number of residents needed to be relocated, and under the comprehensive influence of economic development needs, by 2020, the built-up area exceeded the level before the earthquake.

4.2. Land Use Degree Change

Figure 5 shows the spatial pattern distribution of land-use degree before and after the earthquake at the township scale in the study area. From 2007 to 2008, due to the impact of the Wenchuan earthquake and secondary disasters, the comprehensive index of land use degree in Wolong Town showed a decreasing trend, and the land use entered a stage of decline, mainly concentrated in the severely affected areas of the study area, and the change rate of the comprehensive index was −0.046%. The comprehensive index of land-use degree in the north, east, and south of the study area showed a slight increase trend, and the regions with large change rates were mainly distributed in Yingxiu Town (3.587%), YinXing Township (1.748%), and Xuankou Town (1.347%) in the east of the study area. Due to geological disasters, some forests, grassland, and cropland in these towns were destroyed and converted into other land types, resulting in a high change rate of land-use degree. From 2008 to 2014, the comprehensive indexes of land-use degree in Yanmen Township, Weizhou Town, and Keku Township increased due to the decrease in bare land and reconstruction after the earthquake. The change rates were 0.384%, 0.695%, and 1.132%, respectively. These towns are located in the northeast of the study area, and their economic development level is relatively good, which is of great help to the reconstruction and construction after the earthquake. From 2014 to 2020, the comprehensive indexes of land-use degree in towns and townships are basically in the rising development stage. The regions with large change rates of the comprehensive indexes are mainly distributed in Gengda Town and Keku Township, with change rates of 0.520% and 0.464%, respectively. This is mainly due to the increase in built-up and cropland area and the decrease in bare land area. The natural restoration of vegetation and the construction of urbanization are conducive to the improvement of land use degree, and the ecological system of each township gradually tends to have a stable development.

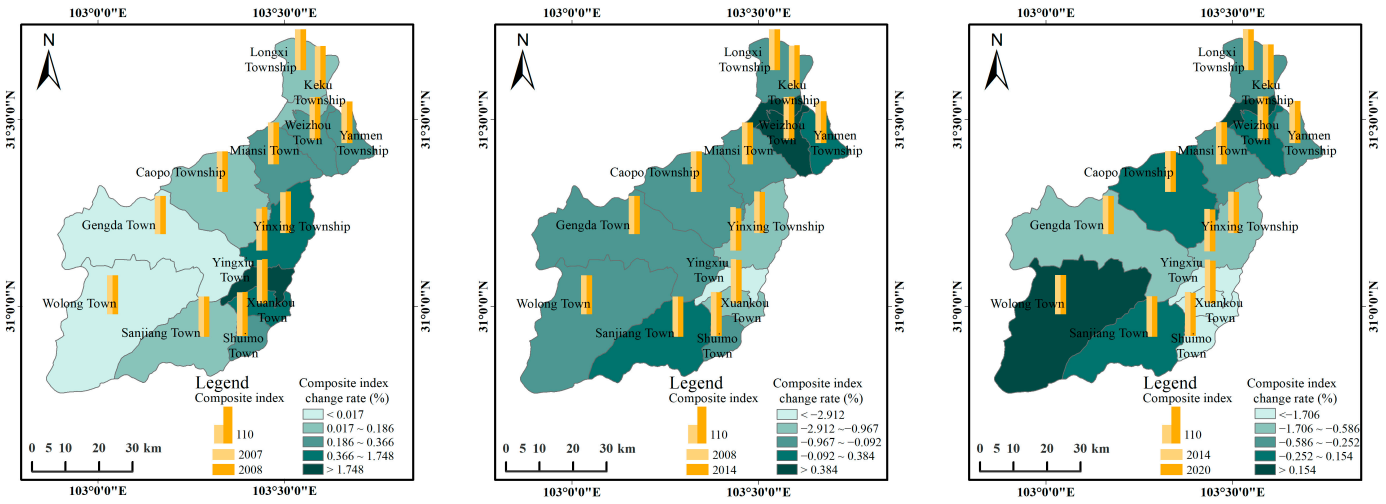

Figure 5. Spatial distribution of land use degree change before and after earthquake.

4.3. Land Use Transfer

Tables 3–5 show the mutual transfer of land use types before and after earthquakes in the study area during 2007–2008, 2008–2014, and 2014–2020, respectively. From 2007 to 2008, all surface cover types in the study area were transferred and transferred out. Due to the "5·12" Wenchuan earthquake, the natural surface was damaged, and a large area was transferred out of the forest, with an area of 33.48km^2. The transfer volume of cropland, grassland, and bare land is relatively large, and the transfer areas are 33.70 km^2, 6.95 km^2, and 4.88 km^2, respectively.

Table 3. Land Use Transfer Matrix for 2007–2008 (km^2).

2007 Year	2008 Year							
	Cropland	**Forest**	**Shrub**	**Grassland**	**Water**	**Snow/Ice**	**Bare Land**	**Built-Up**
Cropland	132.2019	1.4679	0.0306	1.9737	0.4653	0	0	0.5229
Forest	31.9095	2888.4726	1.5624	0	0	0	0	0.0045
Shrub	0.6444	0.1359	10.4697	0.8748	0	0	0	0
Grassland	1.1475	0.8847	0.3528	814.122	0.2223	0	2.9772	0.0306
Water	0	0.0783	0	1.6227	45.324	0	0.8343	0.0657
Snow/Ice	0	0	0	0.018	0.2124	23.9256	1.0683	0
Bare land	0	0.0009	0	2.4597	0.0162	0.2214	107.172	0.0018
Built-up	0	0	0	0	0.1854	0	0	5.6385

Table 4. Land Use Transfer Matrix for 2008–2014 (km^2).

2008 Year	2014 Year							
	Cropland	**Forest**	**Shrub**	**Grassland**	**Water**	**Snow/Ice**	**Bare Land**	**Built-Up**
Cropland	117.4392	32.1714	4.3857	9.3627	0.5049	0	0	2.0394
Forest	22.3587	2848.527	18.8721	1.2114	0.0027	0	0	0.0684
Shrub	1.3383	0.8451	6.2514	3.9807	0	0	0	0
Grassland	6.21	2.5173	0.9225	786.6891	1.3491	0.1071	23.1138	0.162
Water	0.0459	0.2808	0.0621	7.2072	34.56	0.045	3.9258	0.2988
Snow/Ice	0	0	0	0.2898	0.5724	19.4283	3.8556	0.0009
Bare land	0.009	0.0054	0.0018	10.7424	0.7245	7.8831	92.628	0.0576
Built-up	0	0	0	0	0.2025	0	0	6.0615

Table 5. Land Use Transfer Matrix for 2014–2020 (km^2).

2014 Year	2020 Year							
	Cropland	**Forest**	**Shrub**	**Grassland**	**Water**	**Snow/Ice**	**Bare Land**	**Built-Up**
Cropland	106.9065	30.915	2.6271	6.6843	0.063	0	0	0.2052
Forest	11.1924	2862.4914	9.9657	0.6885	0	0	0	0.009
Shrub	1.2294	5.2173	19.0656	4.9761	0.0009	0	0.0063	0
Grassland	7.9902	2.3553	0.5031	782.613	4.8186	0.153	20.9754	0.0747
Water	0.0675	0.0351	0.0108	4.7718	28.9503	0.0126	3.8709	0.1971
Snow/Ice	0	0	0	0.4401	0.5598	19.5336	6.93	0
Bare Land	0.0243	0.0135	0.0027	21.7674	1.2042	7.5366	92.9475	0.027
Built-up	0	0	0	0	0.0684	0	0	8.6202

From 2008 to 2014, the regional ecological environment was restored to a certain extent. During this period, cropland, forest, grassland, and bare land were mainly transferred out, with a total area of 48.46 km^2, 42.51 km^2, 34.38 km^2, and 19.42 km^2, respectively. The bare land type was mainly transferred out to the grassland type. With the development of urban and rural reconstruction, the area of built-up has been transferred to 2.62 km^2, of which the cropland is the main type, and the transferred area is 2.04 km^2. From 2008 to 2014, with the

gradual recovery of vegetation, there was a large amount of conversion of the forest type area, mainly cropland, with a transfer area of 32.17 km^2.

From 2014 to 2020, the cropland, grassland, and bare land had a large amount of transferable areas, which are 40.49 km^2, 36.87 km^2, and 30.58 km^2, respectively. Forest and grassland were transferred in a large amount, with an area of 38.54 km^2 and 39.33 km^2, respectively, indicating that with the passage of time, land use has been continuously improved, vegetation has been restored well, and the overall ecological environment is on the rise under the action of artificial measures and natural restoration.

4.4. Spatial–Temporal Evolution of Landscape Pattern

4.4.1. Temporal Variation Characteristics of Landscape Index

Figure 6 shows the temporal variation trend of the landscape patch density index before and after the earthquake. Compared with 2007, the PD of most landscape types in the study area showed an increasing trend after the earthquake, indicating that the degree of regional landscape fragmentation was intensified, landscape heterogeneity was increased, and the ecological environment was significantly worse due to the earthquake. From 2008 to 2014, the PD values of cropland, shrub, and grassland types changed dramatically, indicating that regional landscape fragmentation caused by earthquakes and secondary geological disasters was serious. PD values of forest and bare land landscape types decreased, indicating that vegetation recovery was good during this period. From 2014 to 2020, the regional PD value basically decreased slightly compared with the previous period. The PD of the built-up type increased slightly, which may be related to the mass production and construction activities carried out during this period. In conclusion, affected by earthquakes and secondary geological disasters, the PD values of all landscape types in the study area changed strongly, especially bare land and some vegetation types, which should be paid more attention to in future ecological environment restoration.

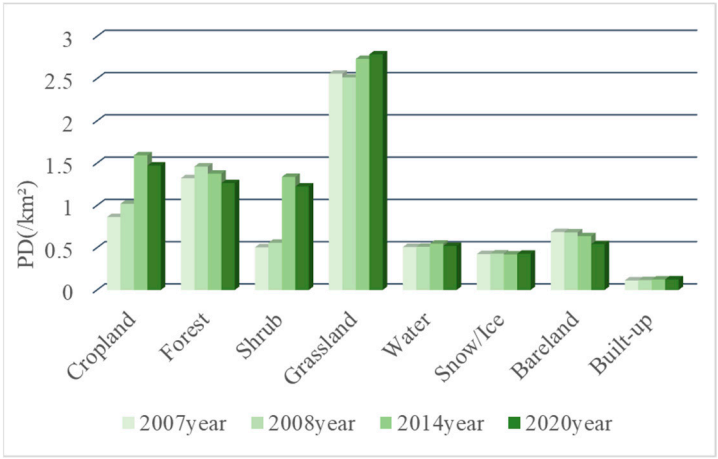

Figure 6. Temporal variation trend of PD index before and after earthquake.

Figure 7 shows the temporal variation trend of the landscape shape index before and after the earthquake. After the 2008 earthquake, the LSI index of all landscape types increased compared with that of 2007, among which the LSI value of cropland, shrub, and bare land changed significantly, indicating that the regional landscape shape was complicated due to the earthquake and secondary geological disasters, and at the same time, it reflected the large intervention of human activities. From 2008 to 2014, LSI values of cropland and shrub types increased most obviously, and landscape shape was still in a relatively complex state. From 2014 to 2020, the LSI value of all landscape types basically decreased compared with that of 2008–2014, and the complex landscape shape gradually returned to the simple situation, while the LSI value of the built-up increased slightly,

which may be due to the relocation of land after the earthquake and the implementation of industrial park projects, which further increased the built-up type.

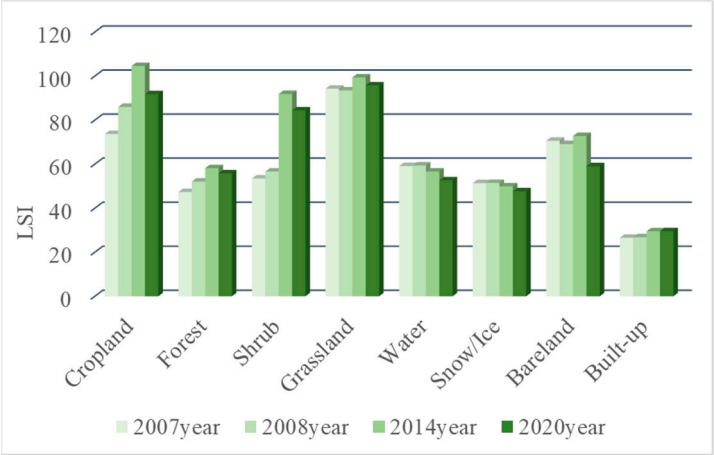

Figure 7. Temporal variation trend of LSI index before and after earthquake.

Figure 8 shows the temporal variation trend of the landscape aggregation index before and after the earthquake. Before the earthquake, the aggregation degree of various landscape patches in the study area was at a high level, and the aggregation degree of forest land was the largest, reaching 97.43, which dominated the AI of the whole region. The AI values of landscape types showed a downward trend from 2007 to 2008, indicating that the connectivity between landscape patches was low and patches were discrete. From 2008 to 2020, most of the landscape classes AI increased significantly, the bare land and built-up is most obvious, the two strong regional landscape type affected by human activities, show that artificial restoration measures of ecological environment recovery has a positive effect, and enable the ecological environment to recover quickly, at the same time it shows that during the earthquake the regional ecological environment experienced benign development.

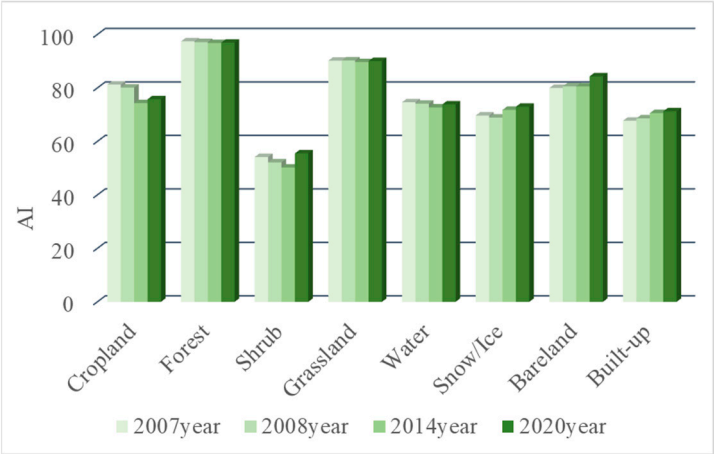

Figure 8. Temporal variation trend of AI index before and after earthquake.

4.4.2. Spatial Variation Characteristics of Landscape Index

Figure 9 shows the spatial distribution of PD before and after the earthquake. The higher PD values before the earthquake were mainly distributed in the west of the study area and around the Minjiang River Basin. After an earthquake in 2008, the maximum PD increased first and then had a decreasing trend; the space change area is still concentrated in the west and around the Minjiang River Basin. The overall change in the landscape pattern

distribution was small, indicating that the degree of regional landscape fragmentation gradually decreased, landscape heterogeneity gradually decreased, and the ecological environment gradually recovered. The PD values in the study area recovered significantly from 2014 to 2020, mainly concentrated around the Minjiang River Basin in the study area, which was closely related to the mass production and construction activities carried out in the later period of earthquake recovery.

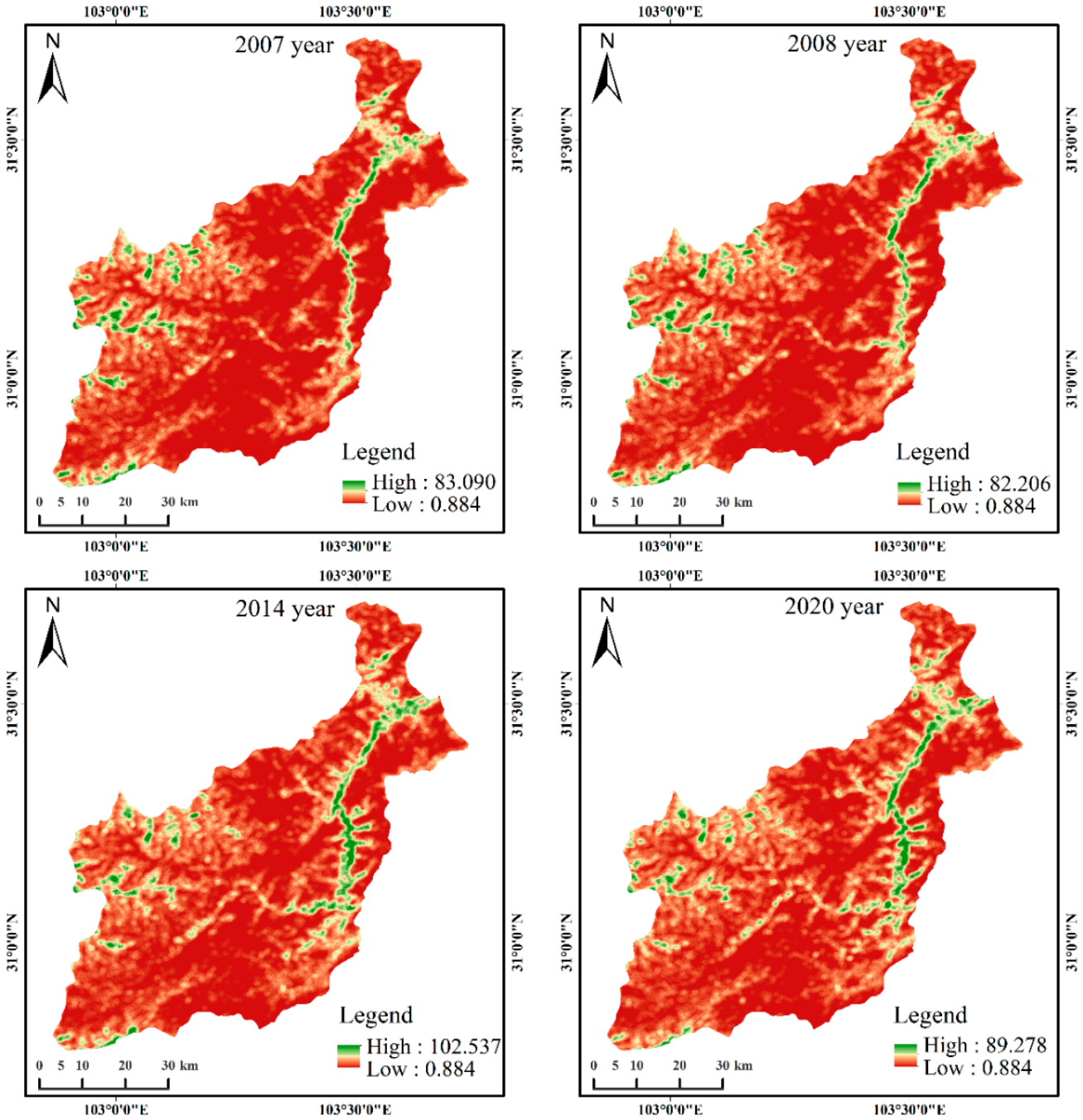

Figure 9. Spatial distribution of PD index before and after earthquake.

Figure 10 shows the spatial pattern distribution of LSI before and after the earthquake. Before the earthquake, the LSI values were mainly distributed in the west and southwest of the study area and around the whole Minjiang River basin. After the 2008 earthquake, the maximum value of LSI increased first and then decreased and basically returned to the level before the earthquake in 2020. Its spatial variation is still concentrated in the

west and southwest of the study area and around the Minjiang River Basin. The results showed that the overall landscape shape complexity recovered well in the late earthquake period; the landscape shape was slightly complicated in the vicinity of the Minjiang River Basin, which may be due to the strong human reconstruction activities and complex surface cover types in the vicinity of Minjiang River Basin, which led to the slow recovery of ecological environment.

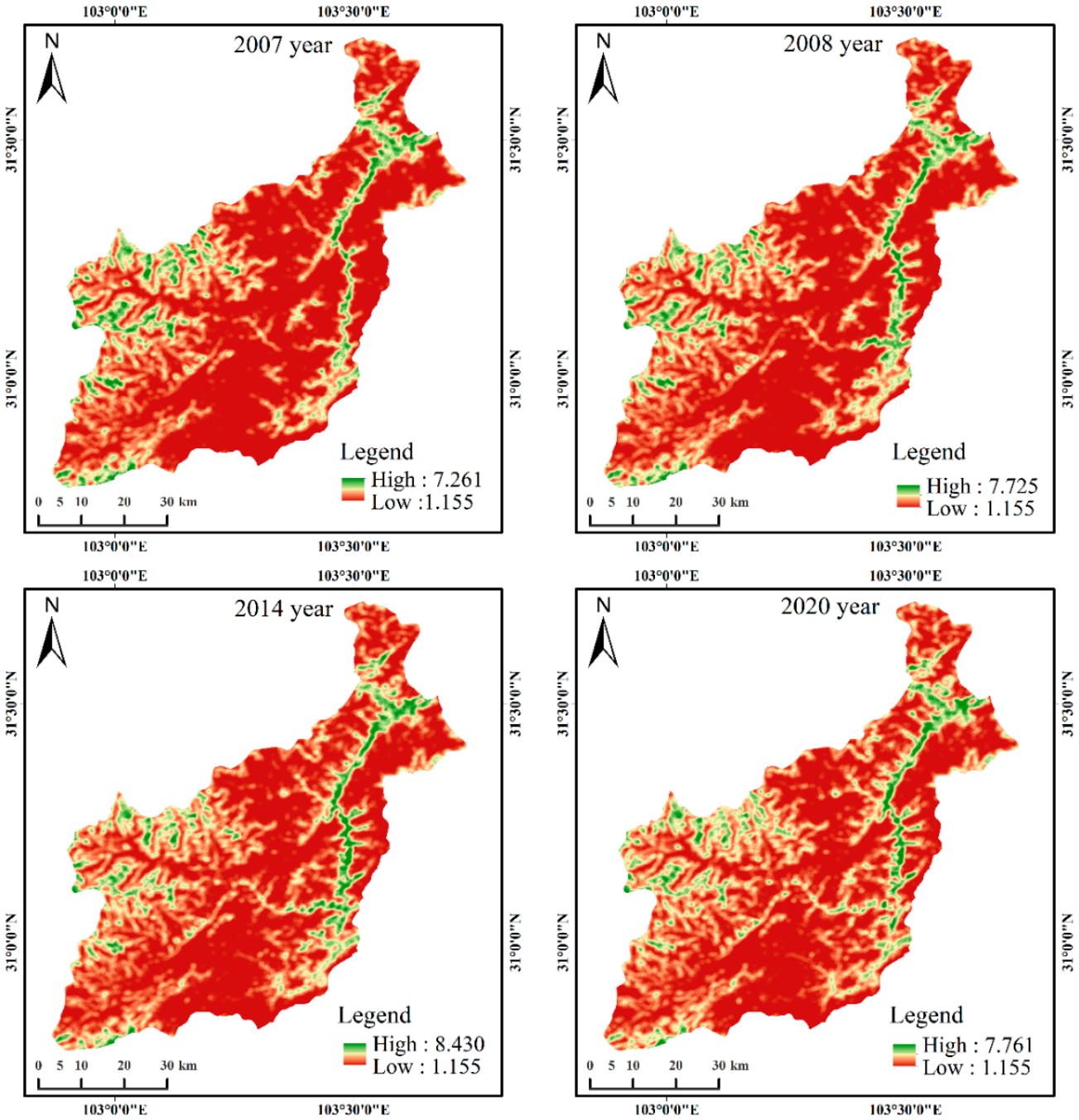

Figure 10. Spatial distribution of LSI index before and after earthquake.

Figure 11 shows the spatial pattern distribution of AI before and after the earthquake. The lower AI values before the earthquake were mainly distributed in the west of the study area and around the whole Minjiang River Basin. After the 2008 earthquake, the minimum value of AI decreased first and then increased, but by 2020, it was still 2.87 lower than that in 2007. From 2008 to 2020, the change in the AI value was mainly concentrated in the

western part of the study area and the whole Minjiang River Basin. The surface landscape in these areas is complex and greatly disturbed by human activities, which makes the recovery of the AI of the affected areas covered by earthquakes and secondary geological disasters slow.

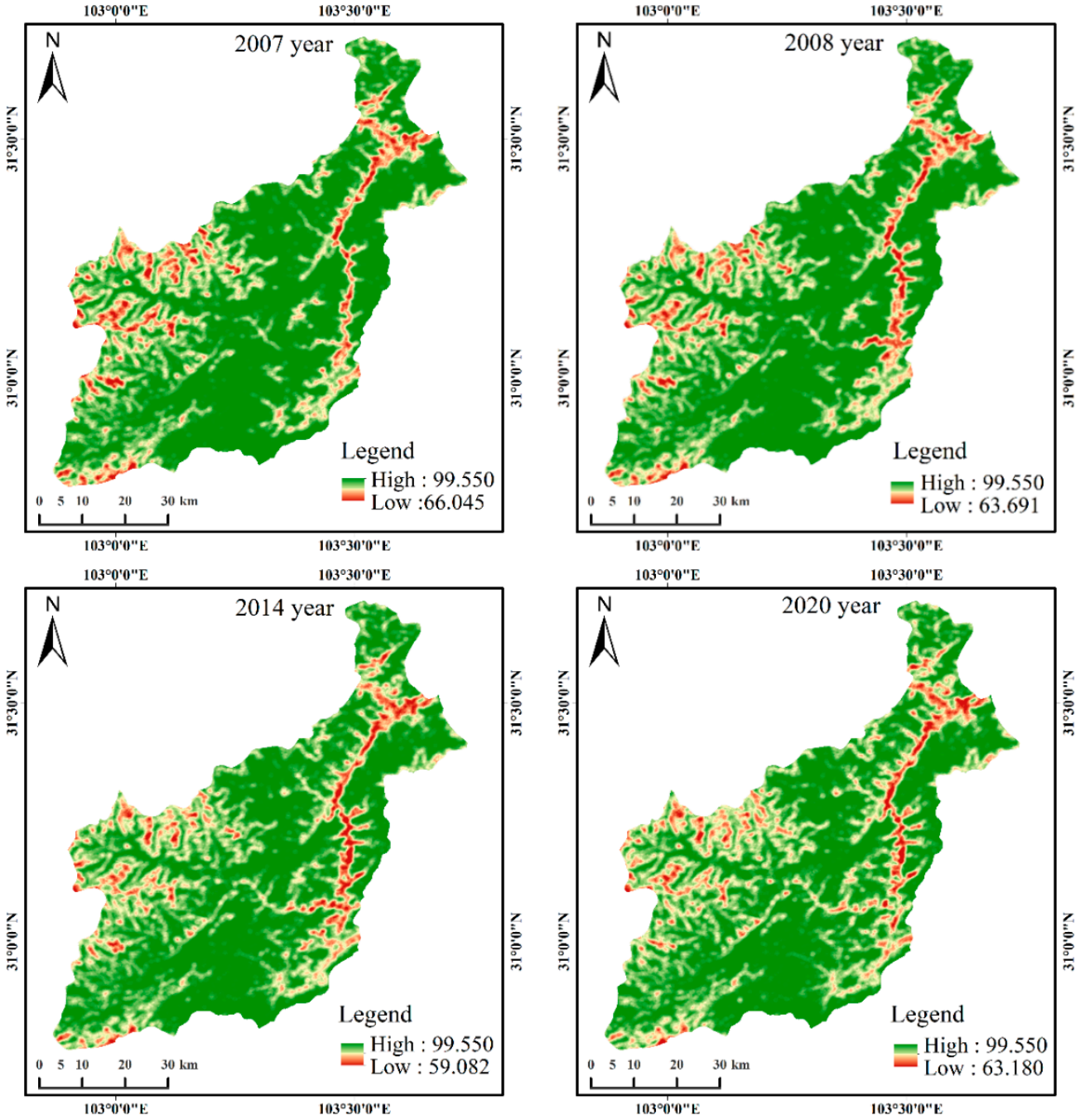

Figure 11. Spatial distribution of AI index before and after earthquake.

4.5. Land Use Change Distribution of Topographic and Geological Conditions

4.5.1. Distribution of Land-Use Change of Different Slope

In order to study the distribution of land-use change under topographic factors, this paper took slope as an example to obtain the slope data of the study area and divided the slope into five grades according to the topography of the study area (<5°, 5–8°, 8–15°, 15°–25°, >25°). Then, the land-use change in the study area was superimposed with the

slope data to analyze the distribution of land-use change before and after the earthquake (2007–2008) (Figures 12 and 13). The results showed that from 2007 to 2008, the largest region of land-use change was mainly distributed in the east and north of the study area, and the slope range was more than 25°. The percentage of the change area to the total change area was 79.10%. The second is the region with a slope of 15–25°, and the percentage of land-use change area in the total change area is 12.97%. The area of land-use change was the smallest in the region, with a slope of 5–8°, and its area percentage was only 1.42%. The reasons for the above phenomenon may be that in the region with a slope of <8°, rivers are the main factors, and land use is not easy to change. Therefore, land-use change in the region with a slope of <8° is small. However, the region with a slope of >25° has complex surface types, such as relatively frequent human activities around cropland and built-up, which will also cause land-use changes. In addition, slope is an important factor leading to landslide and subsequent restoration of land-cover types (especially vegetation) [57,58]. Previous studies have shown that landslides are most likely to occur within a slope range of 20–50° [59,60]. This indicates from the side that the disturbance of earthquakes to surface vegetation is mainly reflected by landslides.

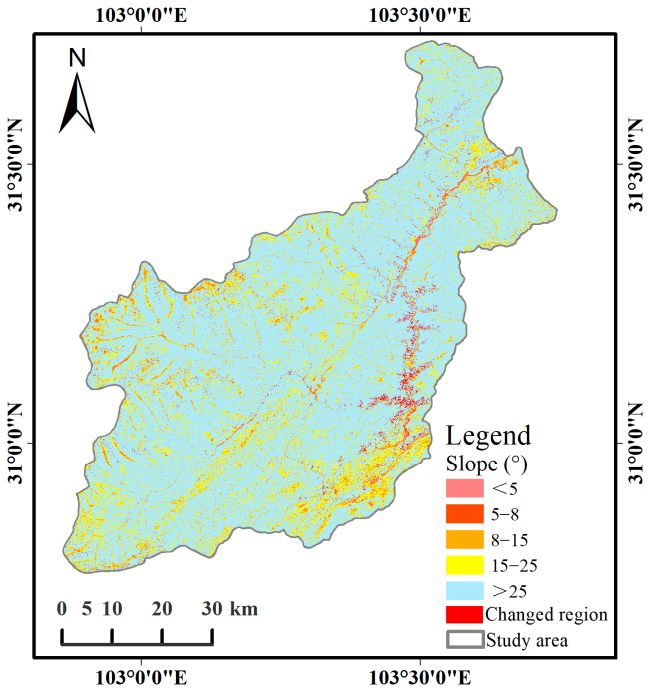

Figure 12. Spatial distribution of land-use change under different slope grades (2007–2008).

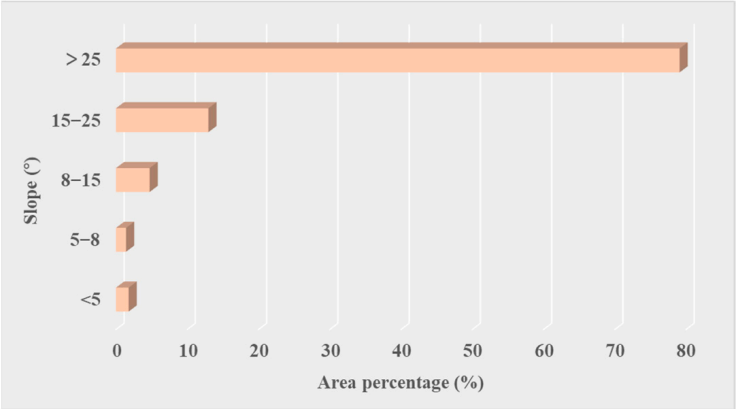

Figure 13. Statistics of land-use change area under different slope grades (2007–2008).

4.5.2. Distribution of Land-Use Change of Wenchuan-Maowen Fault Zone

In this paper, based on the existing research results [61–63], the Wenchuan–Maowen fault zone in the study area was taken as the center to quantitatively express the change rule of land use before and after the earthquake within 5 km and 10 km regions (Figures 14 and 15). The results show that the percentage of land-use change within 5 km of the Wenchuan-Maowen fault zone is 23.23% of the total land-use change area, and the land-use change area is mainly distributed in the northeast of the study area. The percentage of land-use change area within 5–10 km accounted for 19.22% of the total land-use change area, which was mainly distributed in the east and northeast of the study area. The results show that due to the influence of the Wenzhou–Maowen fault zone, the proportion of land-use change in the region closer to the Wenzhou–Mawen fault zone is higher, indicating that the degree of land damage is more serious. Therefore, in the development of land-use resource planning, areas within the fault zone should be avoided in order to reduce the effect of earthquakes on buildings, human life, and property, which cause heavy losses.

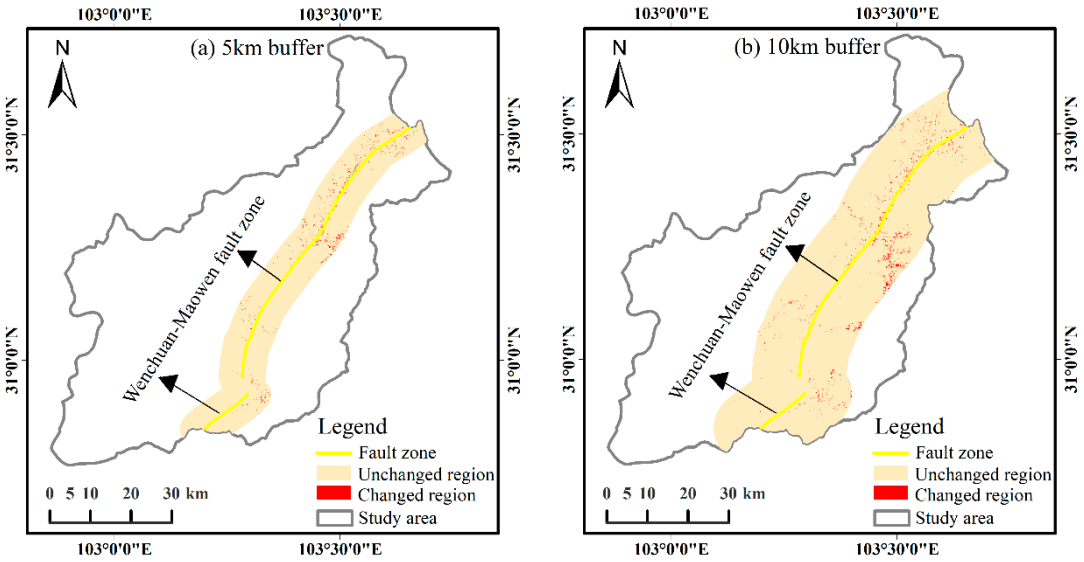

Figure 14. Spatial distribution of land-use change around Wenchuan–Maowen fault Zone (2007–2008).

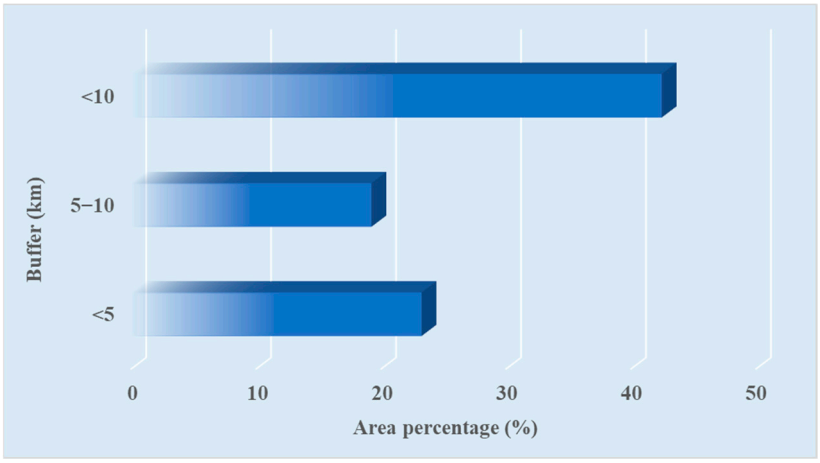

Figure 15. Statistics of land-use change area around Wenchuan–Maowen fault Zone (2007–2008).

5. Discussion

5.1. Geological Hazard Factors Influencing Land Use Change in Earthquake-Stricken Regions

Based on geographical big data, this paper analyzes the spatial–temporal evolution of land use before and after the earthquake in Wenchuan County, the hardest hit area. The

results show that the land use in Wenchuan County has the characteristics of destruction and deformation at both macro and micro scales, which cannot be separated from the natural conditions (such as geological conditions) in the study area.

The area of the cropland, forest, built-up, and bare land types in Wenchuan County changed greatly before and after the earthquake. After the earthquake, the fragmentation degree of most landscape types was aggravated, and the connectivity between landscape patches was low. According to a scientific research report on the 8.0-magnitude Wenchuan earthquake organized by the Monitoring and Forecasting Department of the China Earthquake Administration, the worst-hit areas, such as Yingxiu Town in Wenchuan County, were located near the main surface rupture zone created by the fault zone. However, land surface types such as built-up that straddled earthquake faults were dislocated or seriously damaged by earthquake faults, leading to great changes in the land surface types in Wenchuan County from 2007 to 2008. For example, the bare land area of Wolong Town increased from 46.83 km^2 in 2007 to 48.14 km^2 in 2008.

Based on existing studies [64], geological disasters in Wenchuan County are mainly landslide, collapse, and debris flow. The study area is characterized by large relative height difference, steep terrain slope, vertical and vertical gullies, and large longitudinal ditch ratio drop, which provide basic conditions for the development of geological disasters such as landslide, collapse, and debris flow. The study of Yu [65] et al. showed that the Wenchuan earthquake induced a large number of geological disasters, and the secondary geological disasters were mainly manifested as major landslide disasters, a large number of landslides, and landslide barrier lakes. However, the occurrence of these geological disasters would seriously damage the surface cover information of the study area. The results of this paper show that land use changes greatly in the area with a large slope, mainly because the rock debris in the area with a large slope is more likely to escape from the mountain under the action of gravity, and the river's scour effect on the mountain on both sides increases the instability of the mountain, which is prone to landslides and other geological disasters.

5.2. Human Factors Influencing Land Use Change in Earthquake-Stricken Regions

Government policy guidance is one of the important factors of land-use change; it can guide the change of economic structure, thus indirectly affecting the intensity and mode of land use [66–68]. The decision-making behavior of the government's impact on land-use and cover change is mainly reflected in two aspects: on the one hand is the reasonable adjustment of agricultural production structure, according to local specific circumstances, to the development of fruit trees, Chinese prickly ash as the main economic crops, such an object, which turns parts of cropland to other types of agricultural production, in the process of land-use change from cropland to forest land and other land development. On the other hand, the government's administrative decisions (such as the construction of railways, expressways, etc.) lead to changes in the type and degree of land use [69,70]. From 2007 to 2008, due to the impact of the earthquake, Wenchuan County part of forest and grassland turned into bare land. From 2008 to 2020, due to the relevant policies of Wenchuan County, such as returning farmland to forest, its ecological environment has been continuously improved.

Social and economic development is one of the main reasons affecting land-use change. Economic development is accompanied by the growth of built-up, cropland, and other land types, which will inevitably affect the change of land use structure [71]. Since the reform and opening up, the economy of Wenchuan County has been developing steadily and rapidly [72]. In recent years, it has successively become the first in Aba Prefecture, making an important contribution to the economic development of Aba Prefecture. National Highway 213 and 317 are the main traffic lines in Wenchuan County. The convenience of traffic accelerates the economic development of Wenchuan county and also speeds up the impact on land use. In addition, with an increase in people's ecological consciousness, Wenchuan County adjusted the industrial structure and rational use of land and realized

coordinated development of the economy and environment. The rational use of land resources mainly includes the following aspects: ① Strengthen the protection of cropland and make rational use and development of it and make full use of high-yield arable land to ensure its quality. ② The scientific management of soil and water loss so as to reduce the loss of land resources as far as possible. ③ The study area is rich in tourism resources, and tourism resources can promote not only economic development, but also strengthen environmental protection.

6. Conclusions

Based on geographical big data, this paper explored and analyzed the spatial–temporal evolution characteristics of land use in Wenchuan County before and after the Wenchuan earthquake by using a land use comprehensive degree index, land use transfer matrix, and landscape ecological index. The results show that:

① The area of cropland, forest, built-up and bare land in the study area changed greatly before and after the earthquake. In Yinxing Township, the area of forest changed the most, decreasing from 272.98 km^2 in 2007 to 262.26 km^2 in 2008. By 2020, the area of forest increased to 262.53 km^2 after earthquake recovery. After the earthquake and secondary geological disasters, the comprehensive indexes of land use degree increased slightly in the northern and southern regions of the study area, and the regions with large change rates were mainly distributed in Wolong Town, Keku Township, and Weizhou Town in the eastern part of the study area. From 2014 to 2020, the comprehensive indexes of land-use degree in the study area were basically in the stage of rising development.

② The "5·12" Wenchuan earthquake caused serious damage to the natural surface. From 2007 to 2008, the surface cover types of the study area changed into and out of forest land; the area that turned out to be forest is large, with an area of 33.48 km^2. During the late period of the earthquake, the land use in the study area was improved, and the vegetation was restored well under the action of artificial measures and natural restoration.

③ From the perspective of landscape ecology in the earthquake-stricken regions of land use are analyzed, compared to 2007, most of the landscape in the study area after the earthquake to kind of PD, the LSI value increased, AI basic declining value, shows that the earthquake caused intensified region degree of landscape fragmentation, landscape heterogeneity, low connectivity between landscape patches. After 2008, the PD and LSI values of most landscape types decreased, while AI values increased, indicating that the ecological environment of the whole region showed a benign development in the post-earthquake period.

④ Affected by the slope and the Wenzhou–Maowen fault zone, the proportion of land-use change is higher in the area with a slope of >25° and closer proximity to the Wenzhou–Mawen fault zone, and the degree of land destruction is more serious. Social and economic development and human measures promote the restoration of the regional ecological environment, and government policies, regulations, and policy guidance are the main driving factors affecting the improvement of the regional ecological environment.

Author Contributions: Conceptualization, J.K. and Z.W.; methodology, J.K.; software, J.K., J.W. and X.L.; validation, J.K.; formal analysis, J.K.; investigation, J.K. and Z.W.; resources, H.C. and Z.W.; data curation, H.C. and Z.W.; writing—original draft preparation, J.K.; writing—review and editing, J.K. and Z.W.; visualization, J.K. and J.W.; supervision, H.C. and Z.W.; project administration, H.C. and Z.W.; funding acquisition, Z.W. All authors have read and agreed to the published version of the manuscript.

Funding: This study was supported by the National Key R&D Program of China, Grant No. 2021YFB3900501; the National Natural Science Foundation of China, Grant No. 41901354; the Innovation Project of LREIS, Grant No. O88RAA01YA; the Science and Technology Foundation of the Second Monitoring and Application Center, China Earthquake Administration, Grant No. KJ20220203, and the Science and Technology Foundation of the Second Monitoring and Application Center, China Earthquake Administration, Grant No. KJ20220104.

Data Availability Statement: The data that support the findings of this study are openly available in zenodo at https://zenodo.org/record/4417810#.Yrpa8b1BxPZ, accessed on 6 January 2022.

Conflicts of Interest: The authors declare no conflict of interest. The authors also declare this paper has not been published previously, that it is not under consideration for publication elsewhere, that its publication is approved by all authors, and tacitly or explicitly approved by the responsible authorities where the work was carried out.

References

1. Marano, K.D.; Wald, D.J.; Allen, T.I. Global earthquake casualties due to secondary effects: A quantitative analysis for improving rapid loss analyses. *Nat. Hazards* **2010**, *52*, 319–328. [CrossRef]
2. Wang, Z. A preliminary report on the Great Wenchuan Earthquake. *Earthq. Eng. Eng. Vib.* **2008**, *7*, 225–234. [CrossRef]
3. Ye, S.; Zhai, G.; Hu, J. Damages and lessons from the Wenchuan earthquake in China. *Hum. Ecol. Risk Assess.* **2011**, *17*, 598–612. [CrossRef]
4. Subedi, S.; Chhetri, M.B.P. Impacts of the 2015 Gorkha earthquake: Lessons learnt from Nepal. In *Earthquakes-Impact, Community Vulnerability and Resilience*; IntechOpen: London, UK, 2019.
5. Hu, K.; Zhang, X.; You, Y.; Hu, X.; Liu, W.; Li, Y. Landslides and dammed lakes triggered by the 2017 Ms6. 9 Milin earthquake in the Tsangpo gorge. *Landslides* **2019**, *16*, 993–1001. [CrossRef]
6. Li, C.; Wang, M.; Liu, K. A decadal evolution of landslides and debris flows after the Wenchuan earthquake. *Geomorphology* **2018**, *323*, 1–12. [CrossRef]
7. Meng, X.; Xie, Y.; Bian, F. Distributed Geospatial Analysis through Web Processing Service: A Case Study of Earthquake Disaster Assessment. *J. Softw.* **2010**, *5*, 671–679. [CrossRef]
8. Sun, T.; Davis, E.E.; Wang, K.; Jiang, Y. Trench-breaching afterslip following deeper coseismic slip of the 2012 Mw 7.6 Costa Rica earthquake constrained by near-trench pressure and land-based geodetic observations. *Earth Planet. Sci. Lett.* **2017**, *479*, 263–272. [CrossRef]
9. Elliott, J. Earth Observation for the assessment of earthquake hazard, risk and disaster management. *Surv. Geophys.* **2020**, *41*, 1323–1354. [CrossRef]
10. Xiang, M.; Deng, Q.; Duan, L.; Yang, J.; Wang, C.; Liu, J.; Liu, M. Dynamic monitoring and analysis of the earthquake Worst-hit area based on remote sensing. *Alex. Eng. J.* **2022**, *61*, 8691–8702. [CrossRef]
11. Xiang, H.; Ma, Y.; Zhang, R.; Chen, H.; Yang, Q. Spatio-Temporal Evolution and Future Simulation of Agricultural Land Use in Xiangxi, Central China. *Land* **2022**, *11*, 587. [CrossRef]
12. Luo, L.; Zhou, Q.; He, H.S.; Duan, L.; Zhang, G.; Xie, H. Relative Importance of Land Use and Climate Change on Hydrology in Agricultural Watershed of Southern China. *Sustainability* **2020**, *12*, 6423. [CrossRef]
13. Gao, L.; Ma, C.; Wang, Q.; Zhou, A. Sustainable use zoning of land resources considering ecological and geological problems in Pearl River Delta Economic Zone, China. *Sci. Rep.* **2019**, *9*, 16052. [CrossRef] [PubMed]
14. Li, M.; Cao, X.; Liu, D.; Fu, Q.; Li, T.; Shang, R. Sustainable management of agricultural water and land resources under changing climate and socio-economic conditions: A multi-dimensional optimization approach. *Agric. Water Manag.* **2022**, *259*, 107235. [CrossRef]
15. Huang, Y.; Chen, Z.-X.; Tao, Y.; Huang, X.-Z.; Gu, X.-F. Agricultural remote sensing big data: Management and applications. *J. Integr. Agric.* **2018**, *17*, 1915–1931. [CrossRef]
16. Sajjad, H.; Kumar, P. Future challenges and perspective of remote sensing technology. In *Applications and Challenges of Geospatial Technology*; Springer: Cham, Switzerland, 2019; pp. 275–277.
17. Zhang, B.; Wu, Y.; Zhao, B.; Chanussot, J.; Hong, D.; Yao, J.; Gao, L. Progress and challenges in intelligent remote sensing satellite systems. *IEEE J. Sel. Top. Appl. Earth Obs. Remote Sens.* **2022**, *15*, 1814–1822. [CrossRef]
18. Zhao, S.; Wang, Q.; Li, Y.; Liu, S.; Wang, Z.; Zhu, L.; Wang, Z. An overview of satellite remote sensing technology used in China's environmental protection. *Earth Sci. Inform.* **2017**, *10*, 137–148. [CrossRef]
19. Kang, J.; Yang, X.; Wang, Z.; Cheng, H.; Wang, J.; Tang, H.; Li, Y.; Bian, Z.; Bai, Z. Comparison of Three Ten Meter Land Cover Products in a Drought Region: A Case Study in Northwestern China. *Land* **2022**, *11*, 427. [CrossRef]
20. Kang, J.; Yang, X.; Wang, Z.; Huang, C.; Wang, J. Collaborative Extraction of Paddy Planting Areas with Multi-Source Information Based on Google Earth Engine: A Case Study of Cambodia. *Remote Sens.* **2022**, *14*, 1823. [CrossRef]
21. Wang, J.; Yang, X.; Wang, Z.; Cheng, H.; Kang, J.; Tang, H.; Li, Y.; Bian, Z.; Bai, Z. Consistency Analysis and Accuracy Assessment of Three Global Ten-Meter Land Cover Products in Rocky Desertification Region—A Case Study of Southwest China. *ISPRS Int. J. Geo-Inf.* **2022**, *11*, 202. [CrossRef]
22. Wang, J.; Yang, X.; Wang, Z.; Ge, D.; Kang, J. Monitoring Marine Aquaculture and Implications for Marine Spatial Planning—An Example from Shandong Province, China. *Remote Sens.* **2022**, *14*, 732. [CrossRef]
23. Hakim, W.L.; Lee, C.-W. A review on remote sensing and GIS applications to monitor natural disasters in Indonesia. *Korean J. Remote Sens.* **2020**, *36*, 1303–1322.
24. Zhao, X.; Pan, S.; Sun, Z.; Guo, H.; Zhang, L.; Feng, K. Advances of satellite remote sensing technology in earthquake prediction. *Nat. Hazards Rev.* **2021**, *22*, 03120001. [CrossRef]

25. Kader, A.; Jahan, I. A review of the application of remote sensing technologies in earthquake disaster management: Potentialities and challenges. In Proceedings of the International Conference on Disaster Risk Management, Dhaka, Bangladesh, 12–14 January 2019; pp. 12–14.
26. Li, M.; Tian, S.; Huang, C.; Wu, W.; Xin, S. Risk Assessment of Highway in the Upper Reaches of Minjiang River under the Stress of Debris Flow. *J. Geosci. Environ. Prot.* **2021**, *9*, 21–34. [CrossRef]
27. Li, Q.; Umaier, K.; Koide, O. Research on post-Wenchuan earthquake recovery and reconstruction implementation: A case study of housing reconstruction of Dujiangyan City. *Prog. Disaster Sci.* **2019**, *4*, 100041. [CrossRef]
28. Cui, P.; Zhuang, J.; Chen, X.; Zhang, J.; Zhou, X. Characteristics and Countermeasures of Debris Flow in Wenchuan Area After the Earthquake. *J. Sichuan Univ.* **2010**, *42*, 10–19.
29. Nath, B.; Niu, Z.; Singh, R.P. Land Use and Land Cover changes, and environment and risk evaluation of Dujiangyan city (SW China) using remote sensing and GIS techniques. *Sustainability* **2018**, *10*, 4631. [CrossRef]
30. Yang, W.; Wang, M.; Kerle, N.; Van Westen, C.; Liu, L.; Shi, P. Analysis of changes in post-seismic landslide distribution and its effect on building reconstruction. *Nat. Hazards Earth Syst. Sci.* **2015**, *15*, 817–825. [CrossRef]
31. Wang, M.; Yang, W.; Shi, P.; Xu, C.; Liu, L. Diagnosis of vegetation recovery in mountainous regions after the Wenchuan earthquake. *IEEE J. Sel. Top. Appl. Earth Obs. Remote Sens.* **2014**, *7*, 3029–3037. [CrossRef]
32. Zhang, X.; Wang, M.; Liu, K.; Xie, J.; Xu, H. Using NDVI time series to diagnose vegetation recovery after major earthquake based on dynamic time warping and lower bound distance. *Ecol. Indic.* **2018**, *94*, 52–61. [CrossRef]
33. Liu, X.; Jiang, W.; Li, J.; Wang, W. Evaluation of the vegetation coverage resilience in areas damaged by the Wenchuan earthquake based on MODIS-EVI data. *Sensors* **2017**, *17*, 259. [CrossRef]
34. Tralli, D.M.; Blom, R.G.; Zlotnicki, V.; Donnellan, A.; Evans, D.L. Satellite remote sensing of earthquake, volcano, flood, landslide and coastal inundation hazards. *ISPRS J. Photogramm. Remote Sens.* **2005**, *59*, 185–198. [CrossRef]
35. Balamurugan, G.; Aravind, M. Land use land cover changes in pre-and post-earthquake affected area using Geoinformatics–Western Coast of Gujarat, India. *Disaster Adv.* **2015**, *8*, 1–14.
36. Thilagavathi, N.; Subramani, T.; Suresh, M. Land use/land cover change detection analysis in Salem chalk hills, South India using remote sensing and GIS. *Disaster Adv.* **2015**, *8*, 44–52.
37. Ishihara, M.; Tadono, T. Land cover changes induced by the great east Japan earthquake in 2011. *Sci. Rep.* **2017**, *7*, 45769. [CrossRef]
38. You, Y.; Huang, Y.; Zhuang, Y. Natural disaster and political trust: A natural experiment study of the impact of the Wenchuan earthquake. *Chin. J. Sociol.* **2020**, *6*, 140–165. [CrossRef]
39. Parsons, T.; Ji, C.; Kirby, E. Stress changes from the 2008 Wenchuan earthquake and increased hazard in the Sichuan basin. *Nature* **2008**, *454*, 509–510. [CrossRef]
40. Dai, F.; Xu, C.; Yao, X.; Xu, L.; Tu, X.; Gong, Q. Spatial distribution of landslides triggered by the 2008 Ms 8.0 Wenchuan earthquake, China. *J. Asian Earth Sci.* **2011**, *40*, 883–895. [CrossRef]
41. Chen, Y.; Hu, J.; Peng, F. Seismological challenges in earthquake hazard reductions: Reflections on the 2008 Wenchuan earthquake. *Sci. Bull.* **2018**, *63*, 1159–1166. [CrossRef]
42. Peng, Y.; Gu, X.; Zhu, X.; Zhang, F.; Song, Y. Recovery evaluation of villages reconstructed with concentrated rural settlement after the Wenchuan earthquake. *Nat. Hazards* **2020**, *104*, 139–166. [CrossRef]
43. Lu, T.; Zeng, H.; Luo, Y.; Wang, Q.; Shi, F.; Sun, G.; Wu, Y.; Wu, N. Monitoring vegetation recovery after China's May 2008 Wenchuan earthquake using Landsat TM time-series data: A case study in Mao County. *Ecol. Res.* **2012**, *27*, 955–966. [CrossRef]
44. Wu, F.; Yu, B.; Yan, M.; Wang, Z. Eco-environmental research on the Wenchuan Earthquake area using Disaster Monitoring Constellation (DMC) Beijing-1 small satellite images. *Int. J. Remote Sens.* **2010**, *31*, 3643–3660. [CrossRef]
45. Cui, P.; Lin, Y.-M.; Chen, C. Destruction of vegetation due to geo-hazards and its environmental impacts in the Wenchuan earthquake areas. *Ecol. Eng.* **2012**, *44*, 61–69. [CrossRef]
46. Lu, T.; Shi, F.; Sun, G.; Luo, Y.; Wang, Q.; Wu, Y.; Wu, N. Reconstruction of the Wenchuan earthquake-damaged ecosystems: Four important questions. *Chin. J. Appl. Env. Biol.* **2010**, *16*, 301–304. [CrossRef]
47. Yang, J.; Huang, X. The 30 m annual land cover dataset and its dynamics in China from 1990 to 2019. *Earth Syst. Sci. Data* **2021**, *13*, 3907–3925. [CrossRef]
48. Canters, F. Evaluating the uncertainty of area estimates derived from fuuy land-cover classification. *Photogramm. Eng. Remote Sens.* **1997**, *63*, 403–414.
49. Clark, M.L.; Aide, T.M.; Grau, H.R.; Riner, G. A scalable approach to mapping annual land cover at 250 m using MODIS time series data: A case study in the Dry Chaco ecoregion of South America. *Remote Sens. Environ.* **2010**, *114*, 2816–2832. [CrossRef]
50. Kang, J.; Wang, Z.; Sui, L.; Yang, X.; Ma, Y.; Wang, J. Consistency analysis of remote sensing land cover products in the tropical rainforest climate region: A case study of Indonesia. *Remote Sens.* **2020**, *12*, 1410. [CrossRef]
51. Zhu, S.; Wang, H. *Remote Sensing Image Processing and Application*; Science Press: Beijing, China, 2006.
52. Shi, G.; Jiang, N.; Yao, L. Land use and cover change during the rapid economic growth period from 1990 to 2010: A case study of shanghai. *Sustainability* **2018**, *10*, 426. [CrossRef]
53. Gao, P.; Niu, X.; Wang, B.; Zheng, Y. Land use changes and its driving forces in hilly ecological restoration area based on gis and rs of northern china. *Sci. Rep.* **2015**, *5*, 11038. [CrossRef]

54. Shawul, A.A.; Chakma, S. Spatiotemporal detection of land use/land cover change in the large basin using integrated approaches of remote sensing and GIS in the Upper Awash basin, Ethiopia. *Environ. Earth Sci.* **2019**, *78*, 141. [CrossRef]
55. Wang, J.; Sui, L.; Yang, X.; Wang, Z.; Ge, D.; Kang, J.; Yang, F.; Liu, Y.; Liu, B. Economic globalization impacts on the ecological environment of inland developing countries: A case study of laos from the perspective of the land use/cover change. *Sustainability* **2019**, *11*, 3940. [CrossRef]
56. Kang, J.; Sui, L.; Yang, X.; Wang, Z.; Huang, C.; Wang, J. Spatial pattern consistency among different remote-sensing land cover datasets: A case study in Northern Laos. *ISPRS Int. J. Geo-Inf.* **2019**, *8*, 201. [CrossRef]
57. Wang, H.; Sassa, K.; Xu, W. Analysis of a spatial distribution of landslides triggered by the 2004 Chuetsu earthquakes of Niigata Prefecture, Japan. *Nat. Hazards* **2007**, *41*, 43–60. [CrossRef]
58. Chang, K.-T.; Chiang, S.-H.; Hsu, M.-L. Modeling typhoon-and earthquake-induced landslides in a mountainous watershed using logistic regression. *Geomorphology* **2007**, *89*, 335–347. [CrossRef]
59. Huang, R.; Li, W. Analysis of the geo-hazards triggered by the 12 May 2008 Wenchuan Earthquake, China. *Bull. Eng. Geol. Environ.* **2009**, *68*, 363–371. [CrossRef]
60. Khazai, B.; Sitar, N. Evaluation of factors controlling earthquake-induced landslides caused by Chi-Chi earthquake and comparison with the Northridge and Loma Prieta events. *Eng. Geol.* **2004**, *71*, 79–95. [CrossRef]
61. Wang, F.-X.; Zhou, W.-C. The Study on Land Use Changes of Wenchuan Disaster Area based on RS and GIS. In Proceedings of the 2009 2nd International Congress on Image and Signal Processing, Tianjin, China, 17–19 October 2009; pp. 1–5.
62. Wang, L.; Tian, B.; Masoud, A.; Koike, K. Relationship between remotely sensed vegetation change and fracture zones induced by the 2008 Wenchuan earthquake, China. *J. Earth Sci.* **2013**, *24*, 282–296. [CrossRef]
63. Yang, X.; Yang, W.-N.; Li, Y.-H.; Hu, B.-R. Land Use Land Cover Change Analysis after the Earthquake of Wenchuan. In Proceedings of the 2010 International Conference on Multimedia Technology, Hong Kong, China, 24–25 April 2010; pp. 1–4.
64. Chen, J.; Li, J.; Qin, X.; Dong, Q.; Sun, Y. RS and GIS-based Statistical Analysis of Secondary Geological Disasters after the 2008 Wenchuan Earthquake. *Acta Geol. Sin.-Engl. Ed.* **2009**, *83*, 776–785. [CrossRef]
65. Yu, H.; Luo, Y.; Zheng, Z.; Sun, Y.; Ma, Y. Research on the distribution characteristics of secondary geological disasters induced by 5.12 earthquake in Wenchuan county based on RS and GIS. In Proceedings of the Third International Conference on Digital Image Processing (ICDIP 2011), Sichuan, China, 15–17 April 2011; pp. 269–273.
66. Lubowski, R.N.; Bucholtz, S.; Claassen, R.; Roberts, M.J.; Cooper, J.C.; Gueorguieva, A.; Johansson, R.C. *Environmental Effects of Agricultural Land-Use Change: The Role of Economics and Policy*; United States Department of Agriculture (USDA): Washington, DC, USA, 2006.
67. König, H.J.; Schuler, J.; Suarma, U.; McNeill, D.; Imbernon, J.; Damayanti, F.; Dalimunthe, S.A.; Uthes, S.; Sartohadi, J.; Helming, K.; et al. Assessing the impact of land use policy on urban-rural sustainability using the FoPIA approach in Yogyakarta, Indonesia. *Sustainability* **2010**, *2*, 1991–2009. [CrossRef]
68. Hersperger, A.M.; Oliveira, E.; Pagliarin, S.; Palka, G.; Verburg, P.; Bolliger, J.; Grădinaru, S. Urban land-use change: The role of strategic spatial planning. *Glob. Environ. Change* **2018**, *51*, 32–42. [CrossRef]
69. Chen, L.; Zhu, Y. Bridge Design Concept and Innovation of Chengdu-Dujiangyan Intercity Railway-Post Wenchuan Earthquake Reconstruction Project in Sichuan, China. In Proceedings of the 1st International Workshop on High-Speed and Intercity Railways, Shenzhen, China, 19–22 July 2011; pp. 205–216.
70. Ou, J.; Li, H. The regional engineering damage and reconstruction strategy in Wenchuan earthquake of China. *J. Earthq. Tsunami* **2011**, *5*, 189–216. [CrossRef]
71. Kim, J.H. Linking land use planning and regulation to economic development: A literature review. *J. Plan. Lit.* **2011**, *26*, 35–47.
72. Zhang, J.; Cheng, L. Threshold effect of tourism development on economic growth following a disaster shock: Evidence from the Wenchuan earthquake, China. *Sustainability* **2019**, *11*, 371. [CrossRef]